

# Field effects on the electronic and spin properties of undoped and doped graphene nanodots

Huaxiu Zheng\* and Walter Duley

Department of Physics and Astronomy, University of Waterloo, 200 University Avenue West, Waterloo, Ontario, Canada N2L 3G1

(Received 20 June 2008; revised manuscript received 30 August 2008; published 15 October 2008)

We report a spin-polarized density-functional theory study of electric-field effects on the electronic and spin properties of graphene nanodots. Both undoped and graphene nanodots doped with nitrogen and boron are considered. In the presence of nonlocal exchange-correlation interactions, undoped graphene nanodots are found to be half-semiconductors when a weak electric field is applied across the zigzag edge. At high electric fields these graphene nanodots become nonmagnetic semiconductors. When the electric field is applied across the armchair edge, these graphene nanodots maintain an antiferromagnetic ground state with the energy gap strongly dependent on the magnitude of the electric field. For graphene nanodots doped with nitrogen or boron we find that energetically the most favorable state among all possible configurations is the one in which the dopant replaces the carbon atom at the center of the zigzag edge. The substitutional dopant atom at the zigzag edge leads to a spin-polarized half-semiconducting state in which the spin degeneracy is broken. The spin-dependent energy gaps can be tuned within a wide range by applying electric fields. In addition, we find the half-semiconducting state under doping occurs even when the electric field is very strong. This indicates that edge doping can significantly widen the operating range of applied electric fields for spintronic applications because undoped graphene nanodots become spinless semiconductors under certain applied electric fields.

DOI: [10.1103/PhysRevB.78.155118](https://doi.org/10.1103/PhysRevB.78.155118)

PACS number(s): 73.22.-f

## I. INTRODUCTION

Due to their exceptional properties,<sup>1–8</sup> materials of the graphene family including two-dimensional (2D) graphene, one-dimensional (1D) graphene nanoribbons (GNRs), and zero-dimensional (0D) graphene nanodots (GNDs) have been the focus of much recent research attention from both experimental and theoretical points of view.<sup>6–13</sup> The experimental advances of the fabrication of single-layer graphene and quasi-one-dimensional GNRs (Refs. 1–5) also encourage much new research in this field.<sup>3,9–11</sup> What is more exciting is the very recent report of the successful fabrication of graphene quantum dots as small as 20 nm, so that purely graphene-based single-electron transistors can now be constructed and studied.<sup>14</sup>

Both armchair and zigzag GNRs are semiconducting due to edge deformations and the interactions between the ferromagnetically ordered edge states.<sup>11</sup> At the local-density approximation (LDA) level of theory, an *ab initio* density-functional theory (DFT) study showed that zigzag GNRs can be driven into a half-metallic state where metallic electrons with one spin orientation coexist with insulating electrons having the other spin orientation.<sup>12,15–17</sup> Edge oxidization has been shown to enhance the half-metallicity of zigzag GNRs by lowering the critical electric field needed to induce the half-metallic state.<sup>13</sup> A theoretical study on a finite cluster of zigzag GNRs ( $C_{472}H_{74}$ , of length 7.1 nm and width 1.6 nm) at the B3LYP level indicates that the nonlocal exchange interaction removes half-metallicity in finite GNRs.<sup>15</sup> The resulting finite GNRs are spin-selective semiconductors and it is believed that the finite-size effect in finite GNRs induces this difference.<sup>17</sup> In addition, chemical decoration<sup>18</sup> and substitutional doping<sup>19,20</sup> have also been found to be alternative ways to achieve half-metallicity in zigzag GNRs.

In this paper, we present a detailed study of electric-field effects in doped and undoped GNDs (0D counterpart of

GNRs). We also examine differences that occur when the electric field is applied across zigzag and armchair edges. Electronic structures and optimized geometries have been obtained using first-principles DFT spin-unrestricted calculations, implemented with the GAUSSIAN suite of programs.<sup>21</sup> All-electron calculations were carried out with electronic wave functions expanded in a Gaussian-type localized atomic-centered basis set. We have used the hybrid exchange-correlation functionals of Becke, Lee, Yang, and Parr (B3LYP),<sup>22</sup> which was shown to give a good representation of the characteristics of electronic structure in nanoscale C-based systems.<sup>15,17,23</sup> B3LYP by its construction includes nonlocal exchange interaction, which plays an important role in spin systems.<sup>15</sup> We have adopted the 3-21G basis set,<sup>24</sup> which we find to be adequate when considering both computational efficiency and the accuracy of results.<sup>25</sup> Following the previous convention,<sup>16</sup> a  $M \times N$  finite graphene nanodot is defined according to the number of dangling bonds on the armchair edges ( $M$ ) and the number of dangling bonds on the zigzag edges ( $N$ ), as shown in Fig. 1. Electric-field effects were studied by applying electric field along the zigzag edge ( $x$  direction) or along the armchair edge ( $y$  direction).

In Sec. II, we report the influence of applied electric fields on electronic and spin properties of undoped GNDs. In Sec. III, the configuration of singly doped GNDs with one carbon atom substituted by one nitrogen or boron atom has been investigated. In what follows, we still use the term “half-metallic” or “half-semiconducting” to refer to the states having different  $\alpha$  (spin-up) and  $\beta$  (spin-down) electron gaps by following the conventional definition in 1D GNRs.<sup>12,13,19</sup> But we have to keep in mind that 0D GNDs are not exactly “half-metal” or “half-semiconductor” because they are actually finite molecules. The resulting GNDs are half-semiconductors with two separate energy gaps between the highest occupied molecular orbital (HOMO) and the lowest unoccupied molecular orbital (LUMO) for  $\alpha$  and  $\beta$  electrons.

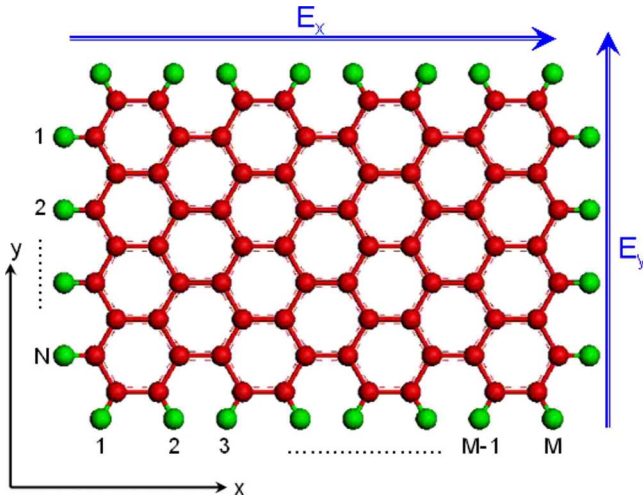


FIG. 1. (Color online) The atomic structure of  $M \times N$  graphene nanodots: the carbon atoms (red) are passivated with hydrogen atoms (green) at both the armchair and zigzag edges. There are  $M$  and  $N$  hydrogen atoms on each armchair edge and zigzag edge, respectively. The applied electric fields (blue arrows) along the armchair and zigzag edges are denoted as  $E_x$  and  $E_y$ , respectively.

This half-semiconducting state is maintained when an electric field is applied along either the  $x$  or the  $y$  direction. Energy gaps are found to be insensitive to the application of an electric field in the  $y$  direction. However, the HOMO-LUMO gap of  $\alpha$  electrons and  $\beta$  electrons tends to vary drastically when an electric field is applied along the  $x$  direction. Such gap modulation is understood from the point of view of the localized or delocalized nature of HOMO and LUMO states. An approximate model is used to estimate the linear-screening factor. A value between 2.12 and 4.24 is obtained, which is in nice agreement with the value of 5 estimated from random-phase approximation (RPA). In addition, we also observe an intriguing symmetry between the field-modulated energy gaps of the donor (N)-doped and acceptor (B)-doped GNDs.

## II. FIELD EFFECT IN UNDOPED GRAPHENE NANODOTS

In this section, we report the results of a study into the effect of applying an electric field in the  $x$  or  $y$  direction, which is across the zigzag edge and across the armchair edge (Fig. 1). By comparing the energy configuration, we found the antiferromagnetic spin singlet ( $S=0$ ) is always the ground state of undoped GNDs with and without electric fields. This is in agreement with previous work by Hod *et al.*<sup>16</sup> Figure 2 shows the calculated spatial distribution of the spin density  $[\rho_\alpha(\mathbf{r}) - \rho_\beta(\mathbf{r})]$  when the electric field is 0.000, 0.082, 0.164, 0.246, and 0.328 V/Å. In the absence of an electric field, the antiferromagnetic ground state has the highest spin density on the zigzag edges and decreases rapidly from the zigzag edge to the middle. This is in agreement with the results of other calculations.<sup>15,16</sup> Application of a weak electric field (0.082 V/Å) slightly changes the spin density. But as the field increases (to 0.162 and 0.246 V/Å), the spin density is

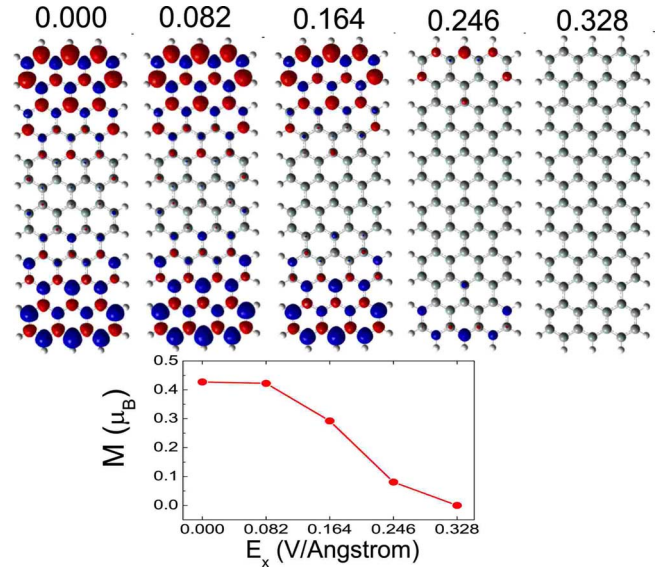


FIG. 2. (Color online) Top: the spin density (difference between  $\alpha$ -spin and  $\beta$ -spin density) map of the antiferromagnetic ground state of  $12 \times 3$  graphene nanodots under cross zigzag edge (along armchair edge) electric field with different strengths, 0.000, 0.082, 0.164, 0.246, and 0.328 V/Å, as labeled above the figures. Red: positive; blue: negative. The isovalue is 0.002. Bottom: the largest local magnetic moment ( $M$ ) of carbon atoms against the applied cross zigzag edge electric field ( $E_x$ ).

dramatically reduced. It is found that spin density completely disappears when the field increases to 0.328 V/Å, resulting in a diamagnetic ground state. Quantitatively, the decrease in the local magnetic moment of carbon atoms ( $M$ ), indicates how an increase in the electric field destroys the spin density configuration, as shown in the bottom of Fig. 2. Without an electric field, the largest magnetic moment of edge atoms  $M=0.43\mu_B$ , which is in nice agreement with the result obtained with the Perdew-Burke-Ernzerhof (PBE) exchange-correlation functional.<sup>26</sup> The disappearance of spin density is attributed to spin transfer between the two zigzag edges induced by the applied electric field.<sup>12</sup> We studied the system with lengths up to 2.5 nm (which is the computational limitation of our method); we do not observe the pattern of spin standing wave reported previously,<sup>15</sup> where the spin density first disappears at the middle of the zigzag edge. We believe this difference occurs because the system that is the subject of the present work is much shorter along the direction of the zigzag-edge direction than those studied by Rudberg *et al.* (0.74 vs 7.1 nm).

The  $\alpha$  and  $\beta$  HOMO-LUMO energy gaps in  $12 \times 3$  GNDs are shown in Fig. 3(a) plotted vs electric-field strength in the  $x$  direction. It can be seen that there are four distinguishable regions of applied electric field: 0–0.10, 0.1–0.27, 0.27–0.46, and 0.46–0.82 V/Å. For fields < about 0.1 V/Å, the electric field causes the  $\alpha$  spin to experience a rapid increase in energy gap, while the  $\beta$  spin experiences a significant decrease in energy gap. At 0.1 V/Å, the  $\alpha$ -spin gap reaches its maximum value and the  $\beta$ -spin gap is minimized. The minimum  $\beta$  energy gap is referred as  $E_m$ . A further increase in field strength is seen to cause the  $\alpha$ -spin gap to decrease while the  $\beta$ -spin gap remains nearly constant until the field

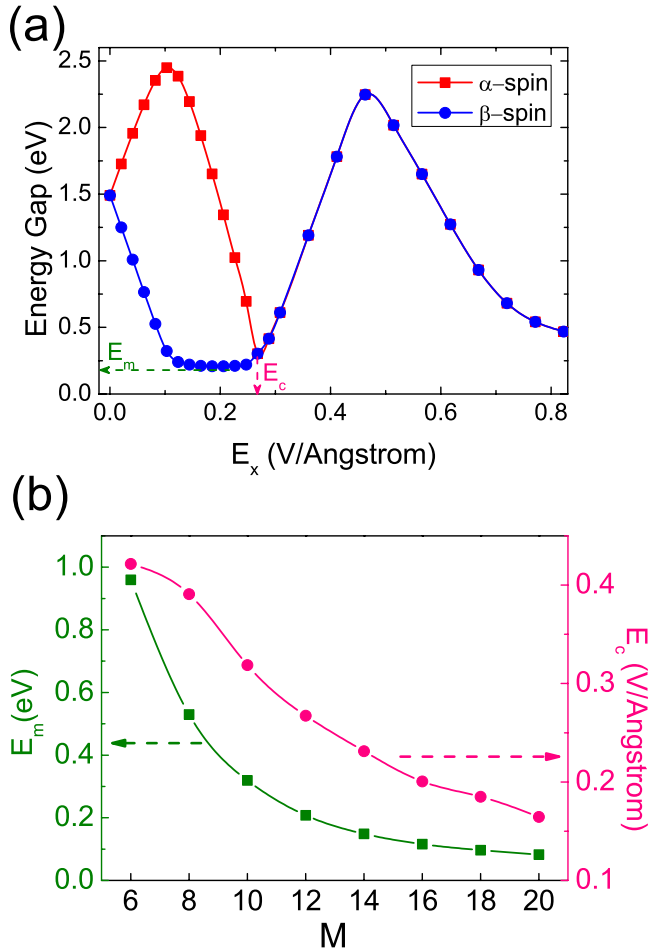


FIG. 3. (Color online) (a) The HOMO-LUMO energy gaps of  $12 \times 3$  GNDs as a function of the strength of  $x$ -direction electric field. Red squares are for  $\alpha$  spin and blue circles are for  $\beta$  spin. The minimal energy gap of  $\beta$  spin ( $E_m$ ) that can be obtained in the whole range of field strength is indicated by an olive dashed arrow. The critical field strength ( $E_c$ ) that will drive the system to be diamagnetic is indicated by a pink dashed arrow. (b) The length dependence of  $E_m$  (left axis) and  $E_c$  (right axis).  $M$  varies from 6 to 20 (a range of length from 11.4 nm to 41.2 nm in  $x$  direction) with fixed length in  $y$  direction ( $N=3$ ). Note that  $M$  is even.

increases to  $0.27$  V/Å. At this point, the field strength is referred to as  $E_c$ . The system is spin-selective half-semiconducting before reaching  $E_c$ .<sup>15</sup> After  $E_c$ , the system becomes diamagnetic and the  $\alpha$  and  $\beta$  electrons have the same gap. The energy gap then increases until the field reaches  $0.46$  V/Å. After  $0.46$  V/Å, the gap decreases rapidly.

The minimal gap  $E_m$  decreases rapidly as the length of GNDs increases in the  $x$  direction as shown in Fig. 3(a). Its value determines how close the corresponding GND approaches to becoming a half-metal with a zero gap. Meanwhile,  $E_c$  is the parameter that defines the operating regime of the spin-selective half-semiconductors since fields in excess of  $E_c$  will destroy the half-semiconducting state. The length dependence of  $E_m$  and  $E_c$  is plotted in Fig. 3(b). An exponential fitting gives  $E_m = A_1 e^{-M/3.06} + A_2$ ,  $A_1 = 6.22$  eV,  $A_2 = 0.08$  eV. On the other hand,  $E_c$  is also a decreasing

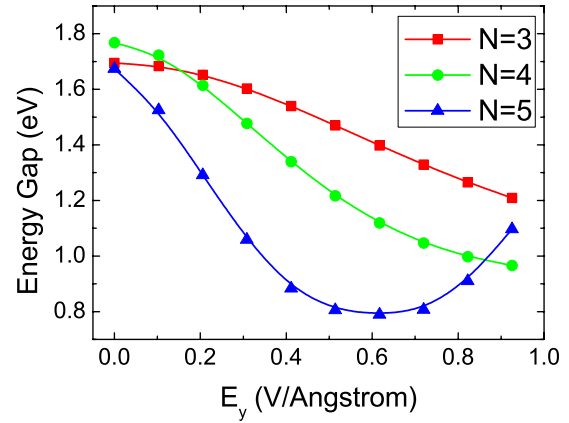


FIG. 4. (Color online) The HOMO-LUMO energy gaps of  $6 \times N$  ( $N=3-5$ ) GNDs as a function of the strength of  $y$ -direction electric field. Red squares are for  $N=3$ , green circles are for  $N=4$ , and blue triangles are for  $N=5$ .

function of length, with an exponential fitting  $E_c = B_1 e^{-M/6.46} + B_2$ ,  $B_1 = 0.91$  V/Å,  $B_2 = 0.12$  V/Å. It is noticeable that the operating regime of field strength for half-semiconducting applications is narrowed for longer GNDs. This limited working range requires special attention in half-semiconducting applications to make sure that the spin state is not destroyed by application of strong fields.

We have also investigated the impact of applying an electric field in the  $y$  direction on the electronic structure of GNDs. The ground state remains antiferromagnetic for  $6 \times N$  ( $N=3-5$ ) GNDs under an applied field in the  $0-1$  V/Å range. The energy gap as a function of field strength is plotted in Fig. 4. For all three cases ( $N=3-5$ ), it was found that for fields less than  $0.5$  V/Å, the HOMO-LUMO energy gap is inversely proportional to field strength. The dependence of the HOMO-LUMO gap on electric field in this range is approximately linear. A similar behavior of field-modulated gap has been found in carbon nanotubes (CNTs) before.<sup>27</sup> The decreasing slope ( $L$ ) is larger for wider GNDs, i.e.,  $L_{N=3} < L_{N=4} < L_{N=5}$  and it is obvious that the field effect is more pronounced in wider GNDs. This is because the same electric field will induce a larger electrostatic potential in wider GNDs. In addition, it should be noted that when  $N=5$  and the field is higher than  $0.6$  V/Å, the energy gap stops decreasing and begins to increase as the field is increased. This minimum actually also appears within  $0-1$  V/Å when  $N > 5$ . The reason we cannot find a minimum for  $N=3,4$  is that at these cases a field higher than  $1$  V/Å is necessary to generate a minimum gap. The increasing behavior of energy gap after the minimum is probably because the system has reached the limit of linear response and nonlinear response makes the gap an increasing function of field.

### III. FIELD EFFECT IN SINGLE N- OR B-DOPED GRAPHENE NANODOTS

Chemical doping is an alternative way to tailor the electronic properties of materials such as CNTs for transport, sensing, and optical applications.<sup>28-30</sup> Boron doping in zig-

zigzag GNRs has been shown to induce a metal-semiconductor transition in the ferromagnetic state and also breaks the spin-up and spin-down symmetry.<sup>31</sup> This work demonstrated that spin-polarized electronic currents can be generated and the resulting GNRs can be used as spin filter devices.<sup>31</sup> Zigzag GNRs can also be tuned to be half-metallic with boron doping on the edges.<sup>20</sup> In addition, nitrogen doping in both armchair and zigzag GNRs has been studied by several research groups.<sup>19,32</sup> However, chemical doping has rarely been studied in GNDs, which are the 0D counterparts of GNRs.

To study the effect of doping with a single nitrogen or boron atom, we have compared the total energies ( $E$ ) for all the possible substitutional sites in a  $6 \times 3$  GND, with edges passivated by hydrogen atoms. As shown in Fig. 5(a), there are 42 carbon atoms in a  $6 \times 3$  GND, but only 12 possible substitutional sites due to the symmetric geometry. A single substitution in a  $6 \times 3$  GND corresponds to a doping concentration of 2.38%. The energy differences between different configurations are listed in Table I for both nitrogen and boron doping. We find that the energetically most favorable doping site for both nitrogen and boron atoms is at site 1 at the center atom of the zigzag edge. We refer to this site as the central zigzag-edge site. The C-N and C-B bond lengths are 1.384 Å and 1.524 Å, respectively. It has been previously reported that for zigzag GNRs boron prefers to substitute at the edge.<sup>31</sup> Thus, it is not surprising that a similar doping preference is observed here since a GND is a finite segment of a zigzag GNR. To verify this result, we also studied a large set of GNDs of different widths and lengths, including  $6 \times N$  ( $N=4-7$ ) and  $M \times 3$  ( $M=8-12$ ) structures and found that central zigzag-edge doping is always the favorable configuration for a single nitrogen or boron substitution. It is then generally expected that a single nitrogen or boron atom should always prefer to replace the central carbon atom of zigzag edge in the actual doping process.

Figure 5(b) shows the DOS for nitrogen- and boron-doped  $6 \times 3$  GNDs as well as for undoped GNDs. Comparison with undoped GNDs indicates that for both nitrogen- and boron-doped GNDs, the spin degeneracy between the  $\alpha$  spin and the  $\beta$  spin is broken. The introduction of one donor (or acceptor) atom leaves one  $\alpha$  (or  $\beta$ ) electron unpaired. The HOMO (LUMO) states of  $\alpha$  and  $\beta$  electrons thus do not have the same energy anymore. Specifically, for nitrogen-doped GNDs, the LUMO level disappears and a new HOMO level arises for  $\alpha$ -spin electrons. For boron-doped GNDs, the HOMO level disappears and a new LUMO level arises for  $\beta$ -spin electrons. Those energy levels are the donor and acceptor impurity levels induced by nitrogen and boron substitutions, respectively. The resulting GNDs are half-semiconductors, in the sense that these are semiconductors having different energy gaps for spin-up and spin-down electrons.

Having explored the geometry and electronic structure of nitrogen- or boron-doped GNDs, we now turn to the effect of an applied electric field on the corresponding half-semiconducting state. We find cross armchair-edge ( $y$  direction in Fig. 1) electric fields have little impact on the electronic structure of doped GNDs. The cross zigzag-edge electric-field effect on the energy gaps of nitrogen- and

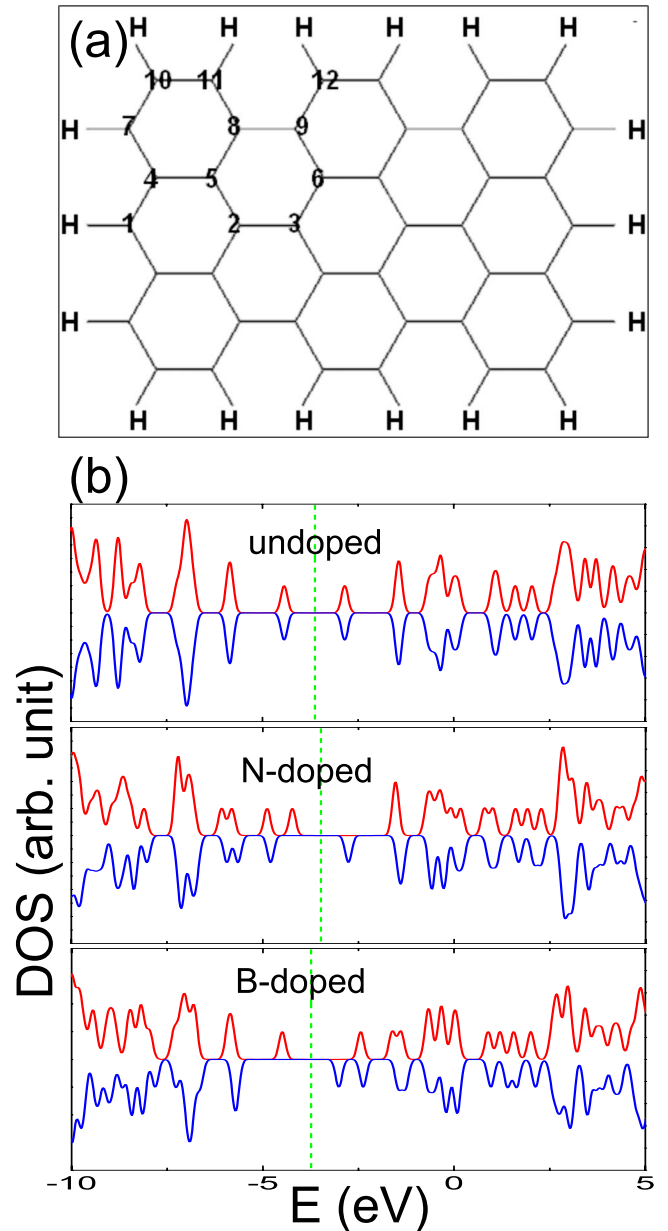


FIG. 5. (Color online) (a) The atomic structure of a  $6 \times 3$  GND and with possible substitutional sites labeled from 1 to 12. (b) Density of states (DOS) in  $6 \times 3$  GNDs without doping, doped with one nitrogen at site 1, and doped with one boron at site 1. Red lines represent the  $\alpha$ -spin channel, while blue lines correspond to the  $\beta$ -spin channel. The Fermi level is indicated by the dashed vertical green line.

boron-doped GNDs is shown in Fig. 6. The half-semiconductivity is retained for fields from  $-1$  to  $1$  V/Å. It is interesting that there is an important donor and acceptor symmetry in the field effect. The gap curve of  $\alpha$  spin in nitrogen-doped GNDs is the mirror image of that of  $\beta$  spin in boron-doped GNDs with respect to the vertical line of zero field. The same symmetry between  $\beta$  spin in nitrogen-doped GNDs and  $\alpha$  spin in boron-doped GNDs is also observed in Fig. 6. In general, when the electric field is applied in the  $x$  or  $-x$  directions, the gap of one spin orientation of N-doped GNDs behaves the same as that of the other spin orientation

TABLE I. Total energy differences for single nitrogen or boron substitution in the  $6 \times 3$  GND:  $\Delta E_{N/B} = E[N_i/B_i] - E[N_1/B_1]$  for  $i = 1 - 12$ .

Configuration	$\Delta E_N$ (eV)	Configuration	$\Delta E_B$ (eV)
N1	0.000	B1	0.000
N2	1.213	B2	0.533
N3	0.828	B3	0.086
N4	1.272	B4	0.670
N5	1.095	B5	0.483
N6	1.381	B6	0.631
N7	0.428	B7	0.372
N8	1.312	B8	0.543
N9	1.051	B9	0.275
N10	1.256	B10	1.240
N11	0.409	B11	0.299
N12	0.952	B12	0.935

of B-doped GNDs when the electric field is reversed. With nitrogen doping, the HOMO-LUMO energy gap for  $\alpha$  spin (2.686 eV) is larger than the one for  $\beta$  spin (2.040 eV) in the absence of electric field. A finite field is necessary to eliminate the gap difference between  $\alpha$  and  $\beta$  electrons. In the presence of a negative field of 0.154 V/Å, the energy gaps for  $\alpha$  and  $\beta$  electrons become nearly the same as indicated by the intersection between the two red lines in Fig. 6. Starting from  $-0.154$  V/Å field, if we apply a more positive field, the energy gap of  $\alpha$  electrons will increase a little and then stays nearly constant after the field reaches a certain strength. However, the gap of  $\beta$  electrons shows a rapid decrease with increasing positive field until about 0.5 V/Å. Conversely, if a negative field greater than  $-0.154$  V/Å is applied, the  $\alpha$  and  $\beta$  gaps show opposite behaviors:  $\beta$  gap

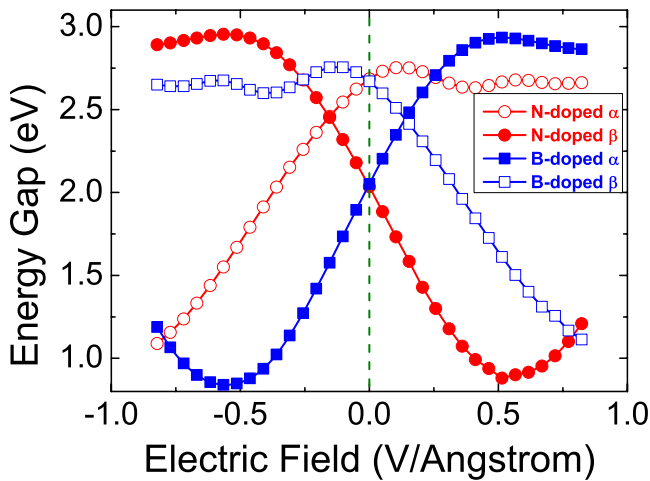


FIG. 6. (Color online) Energy gap as a function of electric field in the  $x$  direction in N- or B-doped  $6 \times 3$  GNDs. A negative field corresponds to the reverse direction. Red empty (filled) circle:  $\alpha(\beta)$  spin of nitrogen-doped GNDs. Blue filled (empty) square:  $\alpha(\beta)$  spin of boron-doped GNDs.

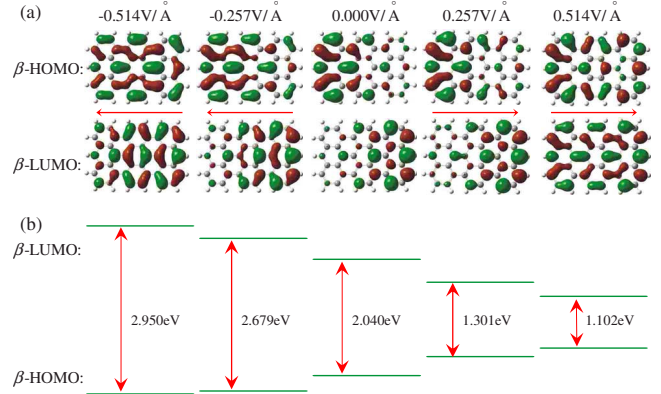


FIG. 7. (Color online) (a) The HOMO and LUMO states of  $\beta$  electrons in N-doped  $6 \times 3$  GNDs under the electric fields:  $-0.514$ ,  $-0.257$ ,  $0.0$ ,  $0.257$ , and  $0.514$  V/Å. Red arrows indicate the direction of the applied field. Color code: red, positive; green, negative. The isovalue is 0.02. (b) The corresponding energy levels of the states shown in (a), with the energy gap indicated.

increases slightly and then remains approximately constant, while the  $\alpha$  gap tends to decrease rapidly. Thus, the same field affects the  $\alpha$  and  $\beta$  gaps in an opposite way.

To explore the mechanism of the gap variation as a function of field strength, the HOMO and LUMO states and energy levels of the  $\beta$  electrons in nitrogen-doped  $6 \times 3$  GNDs at field strengths  $-0.514$ ,  $-0.257$ ,  $0.0$ ,  $0.257$ , and  $0.514$  V/Å are shown in Fig. 7. In the absence of an applied electric field, the  $\beta$ -HOMO state is localized on the right edge, while the  $\beta$ -LUMO state is localized on the left edge. The energy gap between the HOMO and LUMO energy levels is 2.040 eV as indicated in Fig. 7(b). With a negative  $-0.257$  V/Å field applied, the HOMO and LUMO states both remain localized. Consequently, the HOMO energy level is shifted downward and LUMO level is shifted upward by the field because the electrostatic potential  $e\delta V$  is negative on the right edge and positive on the left edge. The HOMO and LUMO levels move apart in energy, leading to an enlarged gap. A larger negative field ( $-0.514$  V/Å) causes the HOMO and LUMO states to become delocalized. Because the electron density is uniformly distributed along the nanodot, the electrostatic potential within the nanodot has both positive and negative components, which compensate each other and together cause slight change in the HOMO-LUMO energy levels and thus the energy gap. As a result, for fields in excess of  $-0.514$  V/Å, the energy gap of  $\beta$  electrons remains nearly constant as shown in Fig. 6. Conversely, a positive field will lift the HOMO level and lower the LUMO level, leaving a narrowed gap. When the electric field exceeds  $0.514$  V/Å, the HOMO and LUMO states become delocalized and the gap stops decreasing. Similar analysis can be made to understand other gap curves as a function of field strength, as long as we know the nature of the state (localized or delocalized). This is because the field can drastically lift or lower the energy levels having localized states, but can only slightly disturb levels corresponding to delocalized states.

In addition, we found that the HOMO-LUMO states of  $\beta$  electrons in N-doped GNDs are always highly localized

when the field is in the range  $-0.2$  to  $0.2$  V/Å. Since HOMO-LUMO states have these characteristics, we can use an approximate model to estimate the screening factor according to the linear dependence of the energy gap on field strength. Electron interactions in graphene are believed to lead to the RPA screening of the external field  $E_{\text{ext}}$ .<sup>33,34</sup> The linear-screening approximation is valid under weak field conditions:<sup>33</sup>  $E = E_{\text{ext}}/k$ , where  $k$  is the screening factor. When the field is between  $-0.2$  and  $0.2$  V/Å, the HOMO and LUMO states are localized on the right and left edges, respectively. The separation distance  $D$  between HOMO and LUMO is approximately between  $4a_c$  and  $8a_c$ , where  $a_c = 1.42$  Å is the standard C-C bond length. The actual electrostatic potential difference between the HOMO and LUMO states induced by field is  $-eED$ . As a result, the energy gap variation ( $\delta E_g$ ) due to the applied field is approximately equal to  $-eED$  since the energy levels are well separated and do not interact strongly under these weak field conditions. Using a linear fit to energy gap ( $E_g$ ) as a function of field strength ( $E_{\text{ext}}$ ) in the range of  $-0.2$  to  $0.2$  V/Å, we obtain  $E_g = aE_{\text{ext}} + b$  and thus  $\delta E_g = aE_{\text{ext}} \approx -eED$ , where  $\delta E_g$  is the gap variation caused by  $E_{\text{ext}}$  compared to the one without electric field. Here,  $a = -2.681$  eÅ,  $b = 2.040$  eV. This results in a linear-screening factor  $k = -eD/a$ , with  $4a_c \leq D \leq 8a_c$ . The value of  $k$  is thus between 2.12 and 4.24, which agrees well with the value  $k = 5$  estimated from the RPA approximation for an infinite graphene sheet<sup>33,34</sup> given the approximations used here.

#### IV. CONCLUSION

In conclusion, it is found that the application of an electric field across the zigzag edges dramatically affects the elec-

tronic and spin properties of undoped and N- or B-doped GNDs. For undoped GNDs, the antiferromagnetic ground state under these conditions becomes half-semiconducting in a weak electric field diamagnetic in strong electric fields. The minimal energy gap that can be obtained within the whole range of field strength decreases rapidly as the length of GNDs increases. As a result, we predict that long GNDs become half-metallic under certain applied electric fields. However, the threshold field under which a GND can be tuned to a diamagnetic semiconductor also decreases with the length of these GNDs. This limits the possible range of electric fields for creation of half-semiconducting GNDs in practical applications. We propose that nitrogen or boron doping can solve this problem because there is an unpaired electron which always gives rise to a half-semiconducting state. By comparing system energies, we find that the most favored configuration is one in which the central carbon atom on the zigzag edge is replaced by a dopant atom. The application of the electric field across the zigzag edges is shown to change the HOMO-LUMO gap of both  $\alpha$  and  $\beta$  electrons. However, an asymmetry in this gap variation is found when applying positive and negative electric fields. This is found to strongly correlate with the localized or delocalized nature of HOMO and LUMO orbitals under applied electric fields. Finally, based on the linear dependence of the energy gap on field strength, we have estimated a linear-screening factor of between 2.12 and 4.24.

#### ACKNOWLEDGMENTS

This research was supported by a grant from the NSERC. This work was made possible by the facilities of the Shared Hierarchical Academic Research Computing Network (SHARCNET: www.sharcnet.ca).

\*Corresponding author; h27zheng@uwaterloo.ca

<sup>1</sup>K. S. Novoselov, A. K. Geim, S. V. Morozov, D. Jiang, Y. Zhang, S. V. Dubonos, I. V. Grigorieva, and A. A. Firsov, *Science* **306**, 666 (2004).

<sup>2</sup>Claire Berger, Zhimin Song, Xuebin Li, Xiaosong Wu, Nate Brown, Cécile Naud, Didier Mayou, Tianbo Li, Joanna Hass, Alexei N. Marchenkov, Edward H. Conrad, Phillip N. First, and Walt A. de Heer, *Science* **312**, 1191 (2006).

<sup>3</sup>M. Y. Han, B. Özyilmaz, Y. Zhang, and P. Kim, *Phys. Rev. Lett.* **98**, 206805 (2007).

<sup>4</sup>B. Özyilmaz, P. Jarillo-Herrero, D. Efetov, D. A. Abanin, L. S. Levitov, and P. Kim, *Phys. Rev. Lett.* **99**, 166804 (2007).

<sup>5</sup>A. L. Vazquez de Parga, F. Calleja, B. Borca, M. C. G. Passeggi, Jr., J. J. Hinarejos, F. Guinea, and R. Miranda, *Phys. Rev. Lett.* **100**, 056807 (2008).

<sup>6</sup>Y. Zhang, Y.-W. Tan, H. L. Stormer, and P. Kim, *Nature (London)* **438**, 201 (2005).

<sup>7</sup>K. S. Novoselov, Z. Jiang, Y. Zhang, S. V. Morozov, H. L. Stormer, U. Zeitler, J. C. Maan, G. S. Boebinger, P. Kim, and A. K. Geim, *Science* **315**, 1379 (2007).

<sup>8</sup>M. I. Katsnelson, K. S. Novoselov, and A. K. Geim, *Nat. Phys.* **2**, 620 (2006).

<sup>9</sup>B. Obradovic, R. Kotlyar, F. Heinz, P. Matagne, T. Rakshit, M. D. Giles, M. A. Stettler, and D. E. Nikonov, *Appl. Phys. Lett.* **88**, 142102 (2006).

<sup>10</sup>Y. Ouyang, Y. Yoon, J. K. Fodor, and J. Guo, *Appl. Phys. Lett.* **89**, 203107 (2006).

<sup>11</sup>Y.-W. Son, M. L. Cohen, and S. G. Louie, *Phys. Rev. Lett.* **97**, 216803 (2006).

<sup>12</sup>Y.-W. Son, M. L. Cohen, and S. G. Louie, *Nature (London)* **444**, 347 (2006).

<sup>13</sup>O. Hod, V. Barone, J. E. Peralta, and G. E. Scuseria, *Nano Lett.* **7**, 2295 (2007).

<sup>14</sup>L. A. Ponomarenko, F. Schedin, M. I. Katsnelson, R. Yang, E. W. Hill, K. S. Novoselov, and A. K. Geim, *Science* **320**, 356 (2008).

<sup>15</sup>E. Rudberg, P. Salek, and Y. Luo, *Nano Lett.* **7**, 2211 (2007).

<sup>16</sup>O. Hod, V. Barone, and G. E. Scuseria, *Phys. Rev. B* **77**, 035411 (2008).

<sup>17</sup>Er-Jun Kan, Zhenyu Li, Jinlong Yang, and J. G. Hou, *Appl. Phys. Lett.* **91**, 243116 (2007).

<sup>18</sup>E. J. Kan, Z. Li, J. Yang, and J. G. Hou, *J. Am. Chem. Soc.* **130**, 4224 (2008).

<sup>19</sup>F. Cervantes-Sodi, G. Csányi, S. Piscanec, and A. C. Ferrari,

- Phys. Rev. B **77**, 165427 (2008).
- <sup>20</sup>S. Dutta and S. K. Pati, J. Phys. Chem. B **112**, 1333 (2008).
- <sup>21</sup>M. J. Frisch *et al.*, GAUSSIAN 03, Revision C.02, Gaussian, Inc., Wallingford, CT, 2004.
- <sup>22</sup>A. D. Becke, J. Chem. Phys. **98**, 5648 (1993).
- <sup>23</sup>S. Yang and M. Kertesz, J. Phys. Chem. A **110**, 9771 (2006).
- <sup>24</sup>K. D. Dobbs and W. J. Hehre, J. Comput. Chem. **8**, 880 (1987).
- <sup>25</sup>P. Shemella, Y. Zhang, M. Mailman, P. M. Ajayan, and S. K. Nayak, Appl. Phys. Lett. **91**, 042101 (2007).
- <sup>26</sup>Oleg V. Yazyev and M. I. Katsnelson, Phys. Rev. Lett. **100**, 047209 (2008).
- <sup>27</sup>J. O’Keeffe, C. Wei, and K. Cho, Appl. Phys. Lett. **80**, 676 (2002).
- <sup>28</sup>H. J. Dai, E. W. Wong, and C. M. Lieber, Science **272**, 523 (1996).
- <sup>29</sup>T. Hasan, V. Scardaci, P. Tan, A. G. Rozhin, W. I. Milne, and A. C. Ferrari, J. Phys. Chem. C **111**, 12594 (2007).
- <sup>30</sup>J. Kong, N. R. Franklin, C. W. Zhou, M. G. Chapline, S. Peng, K. J. Cho, and H. J. Dai, Science **287**, 622 (2000).
- <sup>31</sup>T. B. Martins, R. H. Miwa, A. J. R. da Silva, and A. Fazzio, Phys. Rev. Lett. **98**, 196803 (2007).
- <sup>32</sup>S. S. Yu, W. T. Zheng, Q. B. Wen, and Q. Jiang, Carbon **46**, 537 (2008).
- <sup>33</sup>D. S. Novikov, Phys. Rev. Lett. **99**, 056802 (2007).
- <sup>34</sup>J. Gonzalez, F. Guinea, and M. A. H. Vozmediano, Phys. Rev. B **59**, R2474 (1999).